# A Numerical Approach to Cyclic Consolidation of Saturated Clays

Shay Haq[1], Tian Ho Seah[1], Kuo-Chieh Chao[1], and Cholachat Rujikiatkamjorn[2]
[1]*Department of Civil and Infrastructure Engineering, Asian Institute of Technology, Pathumthani, Thailand*
[2]*School of Civil, Environmental and Mining Engineering, University of Wollongong, Wollongong, Australia*
*E-mail*: 2010civil33@gmail.com

**ABSTRACT:** A finite-difference numerical code is written in MATLAB to predict excess pore pressures and settlements under stepped/square wave cyclic loads. The numerical code is developed by approximating the Terzaghi's 1D consolidation equation under time-dependent loading using the Crank Nicolson scheme. A method of applying the stepped/square wave cyclic loads is proposed. The code considers the nonlinear inelastic stress ~ strain relationship and can be used for both homogeneous and heterogeneous layers. The code is validated by comparing the results with analytical, experimental, and field monitoring data in the literature. A good agreement of the results shows that the code is well developed and can be used in predicting the settlements in practice. The analyses show that the maximum steady-state degree of consolidation calculated based on settlement and the maximum steady-state average degree of consolidation calculated based on dissipation of excess pore pressures decrease as the time period decreases. Below a specific time period, both remain unchanged. For a specific time period, both increase as the percentage of loaded portion in a cycle increases. Besides, the maximum steady-state degree of consolidation based on settlement, for a specific time period, increases with an increase in stress levels, which is due to the nonlinear stress ~ strain behavior.

**KEYWORDS:** Consolidation, Cyclic loads, Finite difference, Crank Nicolson, Settlements.

## 1. INTRODUCTION

In practice, sub-soils underneath structures, including silos and tanks, offshore structures, multistory buildings, road, and rail embankments, are often subjected to cyclic stresses. Engineers have been using the concept of a constant load to predict the consolidation settlements due to cyclic loads, which results in differences between the estimated and the observed settlements. The consolidation behavior of saturated clays under cyclic loads is entirely different from that under a constant load. Positive and negative excess pore-pressures are induced due to loading and unloading, respectively. This can cause water flow out and into the soil mass, thus, making the consolidation process much slower. Also, under cyclic loads, the maximum average degree of consolidation based on dissipation of excess pore pressures never approaches 100% except for very long periods of cyclic loads (Baligh and Levadoux, 1978; Wilson and Elgohary, 1974).

Wilson and Elgohary (1974) presented an analytical solution for consolidation under cyclic loads for highly overconsolidated clays with a constant coefficient of consolidation ($c_v$) for loading and unloading portions. Baligh and Levadoux (1978) put forward the analytical solution for the cyclic consolidation of clays where $c_v$ changes when the stress state of soil shifts from normally consolidated (NC) to over consolidated (OC) or vice versa. Favaretti and Soranzo (1995) considered triangular cyclic loading for OC clays. Toufigh and Ouria (2009) presented an analytical solution using the concept of time transformation technique for the bilinear inelastic model. Matsuda and Shimizu (1995) conducted a laboratory analysis to study cyclic consolidation behavior. Recently, (2018) presented a simplified theoretical solution for the scalene triangular shape cyclic loading, which can better simulate a cereal silo field conditions but assuming a constant $c_v$ during loading and unloading. Terzaghi (1943), Schiffman (1958), and Olson (1977) provided solutions of consolidation with the applied load gradually increasing with time until it reaches a maximum constant value.

If soil's stress state is initially within the NC region, $c_v$ of NC region ($c_v$(NC)) should be used. However, when the applied stress is removed, the effective stresses become lesser than the maximum past stresses, soil rebounds, and enters into the OC region. The cv(OC) is different from that of the NC region. Upon reloading, the soil remains in the OC region until the effective stresses are equal to the maximum past stresses and then enters the NC region again. For the case of highly OC (elastic) clays, $c_v$ remains constant for loading, unloading, and reloading. While for NC and slightly OC clays, soil cyclically shifts from NC to OC state and vice versa; $c_v$ value changes from NC to OC state (Baligh & Levadoux, 1978). The coefficient of consolidation ($c_v$) actually describes the rate at which the consolidation takes place, and its value is higher in the OC range than in the NC range (Duncan, 1993). $c_v$(OC) is about 5 to 10 times the value of $c_v$(NC) (Ladd & Degroot, 2003). A similar observation in the values of $c_v$(NC) and $c_v$(OC) was reported by Seah & Koslanant (2003) for Bangkok soft clay. The value of $c_v$ for a nonlinear soil either increases or decreases with consolidation depending upon the ratio of compressibility to permeability (Indraratna et al., 2016; Walker et al., 2012).

In this paper, the Crank Nicolson solution to Terzaghi's governing differential equation of 1D consolidation under a constant load by Phienwej et al. (2005) is modified to consider the time-dependent loading term. A method of applying the stepped/square wave cyclic loads by using the Terzaghi's equation under time-dependent loading is presented. A computer program is coded in MATLAB, and the verification is made by comparing the results with those of analytical solution by Baligh & Levadoux (1978), experimental analysis results of Toufigh & Ouria (2009), and field monitoring results of a full-scale silo built by Favaretti and Mazzucato (1994) cited in Rahal & Vuez (1998). Moreover, a series of analyses is carried to study the excess pore pressure distribution, the stress-strain behavior under cyclic loads, and the effect of change in time period/frequency and stress levels on the average steady-state degree of consolidation (DOC) calculated based on settlement and dissipation of excess pore pressures.

## 2. GOVERNING EQUATION AND THE NUMERICAL SOLUTION

### 2.1 Governing Equation

Terzaghi's 1D consolidation equation for a homogenous layer under a constant load is written as:

$$\frac{\partial u}{\partial t} = c_v \frac{\partial^2 u}{\partial z^2} \tag{1}$$

For the heterogeneous layer, the above equation can be written as (Phienwej et al., 2005):

$$m_v \gamma_w \frac{\partial u}{\partial t} = \frac{\partial}{\partial z} k \frac{\partial u}{\partial z} \tag{2}$$

For the time-dependent loading, equation 2 can be modified as:

$$\frac{\partial u}{\partial t} = \frac{1}{m_v \gamma_w}\frac{\partial}{\partial z}k\frac{\partial u}{\partial z} + \frac{\partial \sigma}{\partial t} \tag{3}$$

The above equation accounts for the change in the coefficient of permeability (k) with depth.

### 2.2 The Numerical Solution

The finite difference approximation of equation 2 by Crank Nicolson scheme is given as (Phienwej et al., 2005; Premchit, 1978):

$$\frac{(k_i + k_{i-1})}{2}u_{i-1}^{m+1} - \left[\frac{(k_i + k_{i-1})}{2} + \frac{(k_{i+1} + k_i)}{2} + 2m_{vi}\gamma_w\frac{\Delta z^2}{\Delta t}\right] u_i^{m+1} + \frac{(k_{i+1} + k_i)}{2}u_{i+1}^{m+1} = -\frac{(k_i + k_{i-1})}{2}u_{i-1}^{m} + \left[\frac{(k_i + k_{i-1})}{2} + \frac{(k_{i+1} + k_i)}{2} - 2m_{vi}\gamma_w\frac{\Delta z^2}{\Delta t}\right]u_i^m - \frac{(k_{i+1} + k_i)}{2}u_{i+1}^m \tag{4}$$

where, $k_i$ = coefficient of permeability at node "i", $m_{vi}$ = coefficient of volume change at node "i", $u_i^m$ = excess pore pressure at node "i" and time step "m", $\gamma_w$ = unit weight of water,

In Equation 3, the time-dependent loading term was approximated by the first forward difference. Hence, the numerical approximation in Equation 4 can be modified to capture time-dependent loading as (Haq, 2018):

$$-\frac{1}{2m_{vi}\gamma_w}\frac{\Delta t}{\Delta z^2}\frac{(k_i + k_{i-1})}{2}u_{i-1}^{m+1} + \left[\frac{1}{2m_{vi}\gamma_w}\frac{\Delta t}{\Delta z^2}\frac{(k_i + k_{i-1})}{2} + \frac{1}{2m_{vi}\gamma_w}\frac{\Delta t}{\Delta z^2}\frac{(k_{i+1} + k_i)}{2} + 1\right]u_i^{m+1} - \frac{1}{2m_{vi}\gamma_w}\frac{\Delta t}{\Delta z^2}\frac{(k_{i+1} + k_i)}{2}u_{i+1}^{m+1} = \frac{1}{2m_{vi}\gamma_w}\frac{\Delta t}{\Delta z^2}\frac{(k_i + k_{i-1})}{2}u_{i-1}^{m} - \left[\frac{1}{2m_{vi}\gamma_w}\frac{\Delta t}{\Delta z^2}\frac{(k_i + k_{i-1})}{2} + \frac{1}{2m_{vi}\gamma_w}\frac{\Delta t}{\Delta z^2}\frac{(k_{i+1} + k_i)}{2} - 1\right]u_i^m + \frac{1}{2m_{vi}\gamma_w}\frac{\Delta t}{\Delta z^2}\frac{(k_{i+1} + k_i)}{2}u_{i+1}^m + \sigma_i^{m+1} - \sigma_i^m \tag{5}$$

Equation 5 can be solved by matrix inversion technique and written as:

$$\left[u_i^{m+1}\right] = [A]^{-1}[B]\left[u_i^m + \sigma_i^{m+1} - \sigma_i^m\right] \tag{6}$$

where, $u_i^{m+1}$ = excess pore pressures at $i^{th}$ node for current time step "m+1", $u_i^m$ = excess pore pressures at $i^{th}$ node for previous time step "m", [A] = co-efficient matrix of $u_i^{m+1}$, [B] = co-efficient matrix of $u_i^m$, $\sigma_i^{m+1}$ = applied stress at $i^{th}$ node for current time step, $\sigma_i^m$ = applied stress at $i^{th}$ node for the previous time step.

## 3. APPLICATION OF STEPPED/SQUARE WAVE CYCLIC LOAD

Figure 1 shows the stepped/square waves cyclic loading with each loading, and the unloading half-cycle was further divided into several sub-time steps. At the very first sub-time step of the first half loading cycle (1st pulse), both $\sigma_i^{m+1}$ and $\sigma_i^m$ have the same values of applied pressure/stress "q", therefore the term $\sigma_i^{m+1} - \sigma_i^m$ in equation 6 becomes zero. Similarly, on the rest of the first half loading cycle sub-time steps, this term continues to be zero until the first sub-time step of the first half unloading cycle (1st rest period). Hence, Equation 6 for all the sub-time steps of first half loading can be written as:

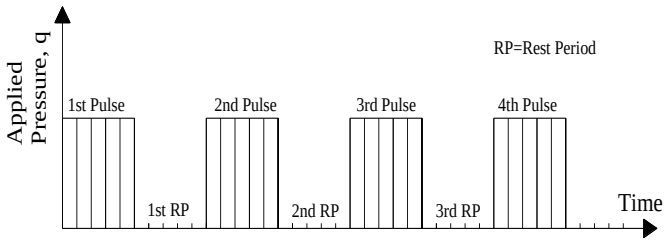


Figure 1 Stepped/Square wave cyclic loading in with each cycle is divided into a number of sub-time steps

$$\left[u_i^{m+1}\right] = [A]^{-1}[B][u_i^m] \tag{7}$$

Equation 7 is the same as that under a constant load, which means that the excess pore pressures for the first loading half-cycle are the same as those under a constant applied load of the same duration.

Now, at the first time step of the first half unloading cycle (1st rest period), $\sigma_i^{m+1}$ becomes zero while $\sigma_i^m$ can have a value equal to the magnitude of applied pressure "q"; therefore, Equation 6 for the first time step of the first half unloading cycle can be written as:

$$\left[u_i^{m+1}\right] = [A]^{-1}[B][u_i^m - q] \tag{8}$$

For the rest of the time steps of the first half unloading cycle (1st rest period), both $\sigma_i^m$ and $\sigma_i^{m-1}$ can have a value equal to zero, and the final equation becomes the same as Equation 7.

Further, at the first sub-time step of the second half loading cycle (2nd pulse), $\sigma_i^{m+1}$ becomes equal to "q" and $\sigma_i^m$ is equal to zero; therefore, the equation becomes:

$$\left[u_i^{m+1}\right] = [A]^{-1}[B][u_i^m + q] \tag{9}$$

For the rest of the sub-time steps of the second-half loading cycle (2nd pulse), the term $\sigma_i^{m+1} - \sigma_i^m$ becomes zero as both $\sigma_i^{m+1}$ and $\sigma_i^m$ are equal to "q" and final equation would be same as Equation 7. Similar procedure can be repeated for the rest of the cycles.

## 4. CHANGE OF STRESS STATE BETWEEN NC AND OC STATES AND THE COMPUTATIONS OF SETTLEMENTS

To consider the stress state between NC and OC state, a conditional statement was applied, i.e., "if the effective stresses are greater than or equal to the maximum past stresses, the soil is in NC state otherwise in OC state."

Three stress-strain models were used (Figure 2) i) linear elastic model for highly OC clays, ii) bilinear inelastic model for NC clays with small stress level (small strains), and nonlinear inelastic model for NC clays with high-stress level (large strains). Using the nonlinear inelastic model, the following equations were used for the calculations of settlements assuming an over consolidation ratio (OCR) = 1:

For the elements with stress state in NC region:

$$S_j^m = CR\log\left(\frac{\sigma'^m_{f_j}}{\sigma'_{v_{oj}}}\right)dH \tag{10}$$

For the elements with stress state in OC region:

$$S_j^m = CR\log\left(\frac{\sigma'^m_{jp}}{\sigma'_{v_{oj}}}\right)dH - RR\log\left(\frac{\sigma'^m_{jp}}{\sigma'^m_{f_j}}\right)dH \tag{11}$$

$$S^m = \sum_{i=1}^{m} S_j^m \qquad (12)$$

where, $S^m$ = settlement of whole layer at time step "m", $S_j^m$ = settlement of $j^{th}$ element at time step "m", $\sigma'^{m}_{p\,j}$ = maximum past stress (pre-consolidation pressure) at $j^{th}$ element until time "m", $\sigma'_{v_{o\,j}}$ = initial effective vertical overburden stress at $j^{th}$ element, $\sigma'^{m}_{f_j}$ = final effective stress at $j^{th}$ element at time step "m", dH = Thickness of the element, CR = compression ratio, RR = recompression ratio.

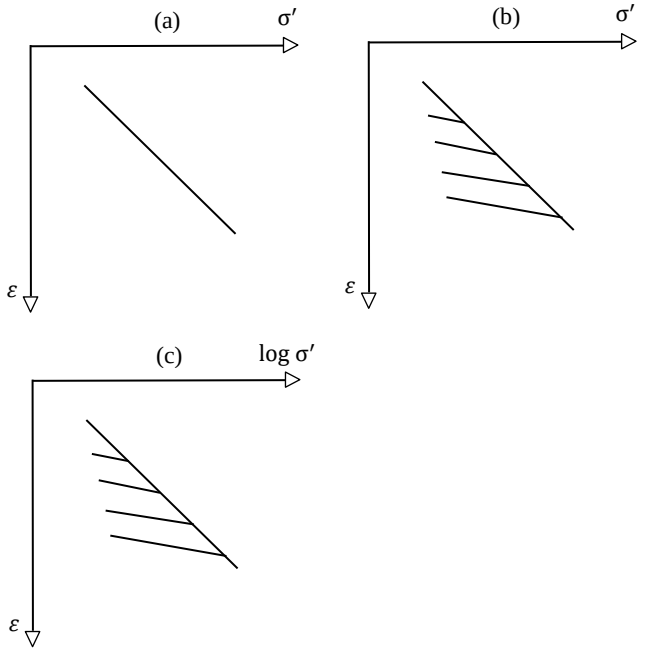


Figure 2 (a) linear elastic model, (b) bilinear inelastic model, (c) non-linear inelastic model

## 5. THE COMPUTER PROGRAM

The computer program is written in MATLAB, and the self-explanatory flow chart of the program is shown in Figure 3. The program considers the nonlinear inelastic model and can efficiently perform the analyses by entering the required input parameters. The input parameters for the program are the thickness of soil layer, time period/frequency of cyclic load, the magnitude of applied external stress, number of elements, time step value, the maximum time for simulation, and soil properties such as compression ratio (CR), recompression ratio (RR) and $c_v$ for both NC and OC regions. The program's outputs are in the form of nodal distribution of excess pore-water pressures, DOC based on dissipation of excess pore pressures, and cumulative settlements with depth.

### 5.1 Assumptions

i. A nonlinear inelastic model is considered.
ii. $c_v$ changes when the soil moves from NC to OC state or vice versa.
iii. The change in the coefficient of permeability (k) with effective stresses is proportional to the change in the coefficient of volume change ($m_v$) with effective stresses; therefore, the $c_v$ value remains constant with consolidation either in NC or OC region, i.e., $c_c/c_k$ =1.0.
iv. Change in $c_v$ is due to change in $m_v$ from NC to OC state or vice versa, i.e., $k_v$ is not affected by over-consolidation; therefore, $\alpha = \beta$.
v. Applied stress is varying with time in the form of square wave/stepped cyclic loading and is kept either constant or varying with depth.

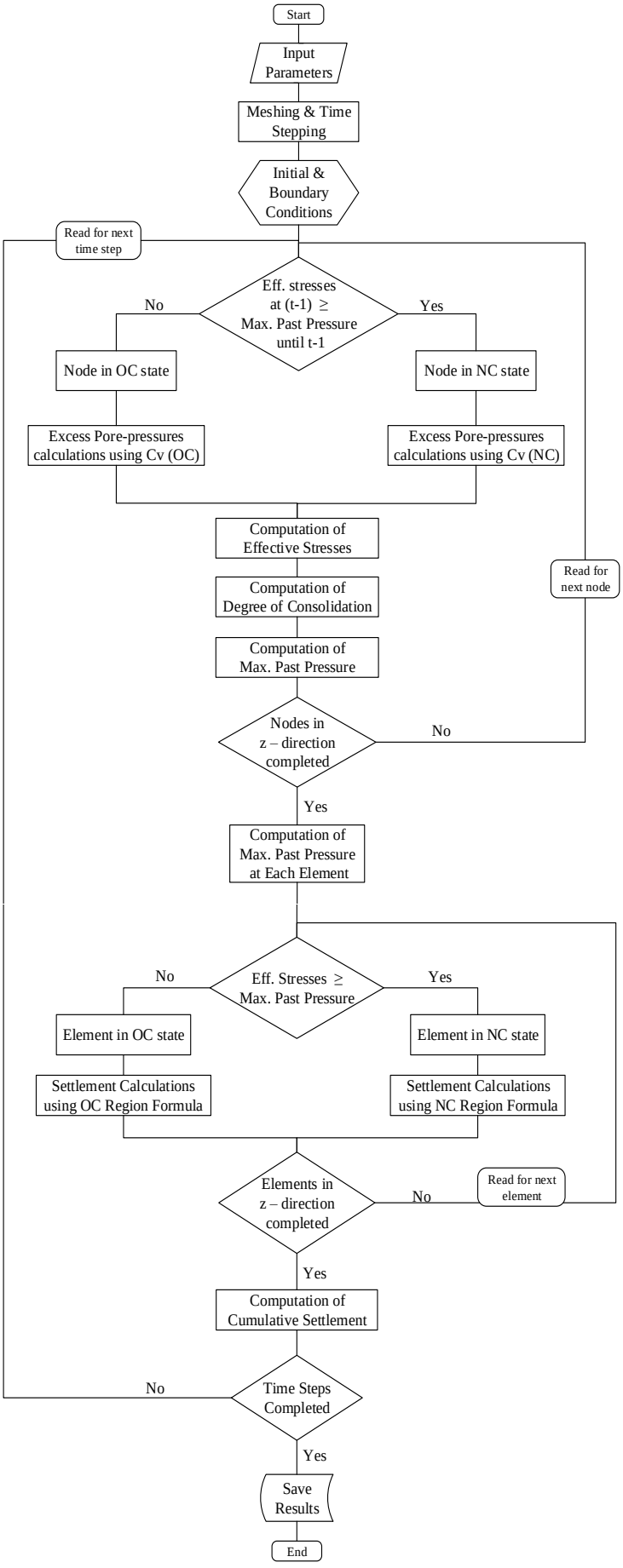


Figure 3 Flow chart of the computer program developed in MATLAB

vi. Soil is considered to be initially in NC state, i.e., OCR = 1.0.
vii. Water and soil grains are incompressible.
viii. Darcy's law is applicable.
ix. Only 1D deformation in the direction of applied external stress can occur.

### 5.2 Validation of the Program

The computer program was validated first by comparing the results to that of the analytical solution by Baligh & Levadoux (1978). Figure 4 shows the comparison of the temporal and spatial distribution of excess pore pressures for a stepped cyclic loading pattern with a time period of 30 days, which could be the case of a silo or an industrial water/oil tank. Fig. 4 shows the results of highly OC clay in which the effective stresses do not exceed the pre-consolidation pressure; hence the $c_v$ remains constant during loading and unloading. The excess pore pressures are positive for the loading half cycles and negative for the unloading half cycles. While the positive excess pore pressures decrease and negative excess pore pressures increase with the number of cycles. After a huge number of cycles, for the case of 50% of loaded portion in a cycle, i.e., X = 0.5 (where "X" is the percentage of loaded portion in a cycle, e.g., for X = 0.25, only 25% of the time period is loaded while the 75% is unloaded), the magnitudes of both positive and negative excess pore pressures are the same with only difference in signs and the magnitude does not change with further increase in the number of cycles. This state is defined as the steady-state.

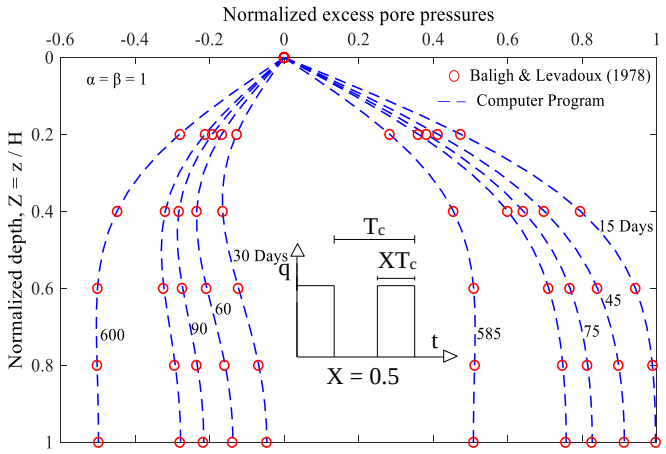


Figure 4 Comparison of the excess pore pressures from the developed computer program and analytical solution by Baligh and Levadoux (1978) for the case of the homogeneous elastic clay layer

Figure 5 shows the comparison results for the case of NC clay. The proposed model's settlement results are compared with that of Baligh and Levadoux's (1978) analytical solution. The comparison results are for the bilinear inelastic model with linear stress versus strain relationship.

The numerical code is also validated by comparing the results to that of experimental/laboratory analysis results by Toufigh & Ouria (2009). They conducted 1D cyclic consolidation tests using twenty (20) oedometer soil samples. Figure 6 shows the comparison results of the maximum average steady-state DOC based on the dissipation of excess pore pressures ($U_{max,\ ss}$) from laboratory analysis and the computer program.

The program was further verified by the field monitoring record of a full-scale silo built in Ca'Mello near Porto Tolle, Italy by Favaretti and Mazzucato (1994) cited in Rahal & Vuez (1998). The silo was built on a 15 m thick layer with top and bottom pervious boundary conditions. The $c_v$ and $m_v$ of the soil layer were 47.3 $m^2$/year and 2.96 x$10^{-4}$ $kPa^{-1}$, respectively. Figure 7 shows the difference in actual and simulated loading types used in the program because the program can apply the stepped/square wave cyclic load.

Figure 8 shows the comparison of the predicted settlements by the program and field monitoring records. The linear elastic model was used for the prediction of the settlements.

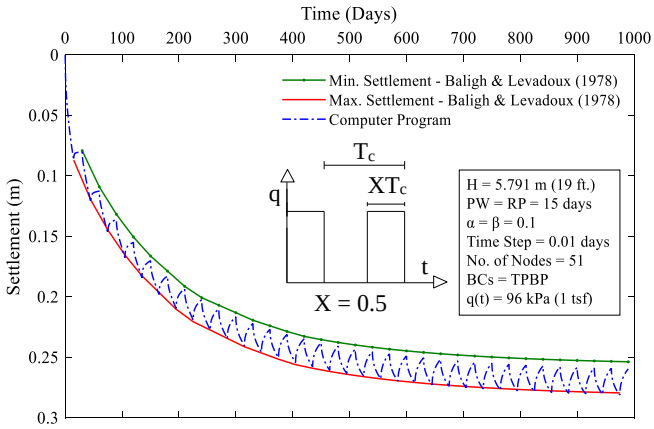


Figure 5 Comparison of the magnitude and history of settlements at the surface from the developed computer program and analytical solution for the case of homogeneous NC clay layer

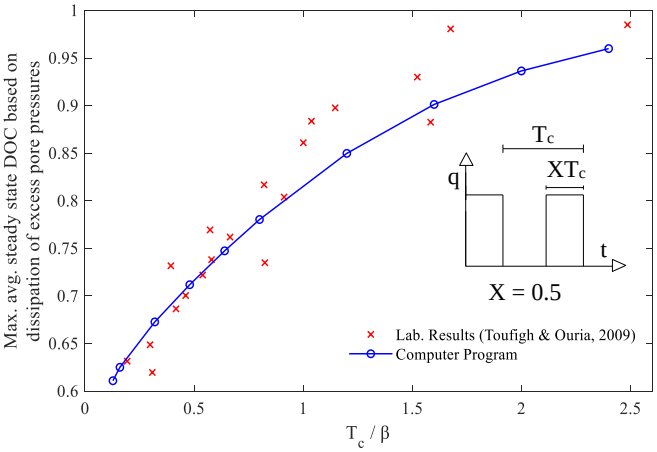


Figure 6 Verification of the results of the computer program with laboratory analysis results by Toufigh and Ouria (2009)

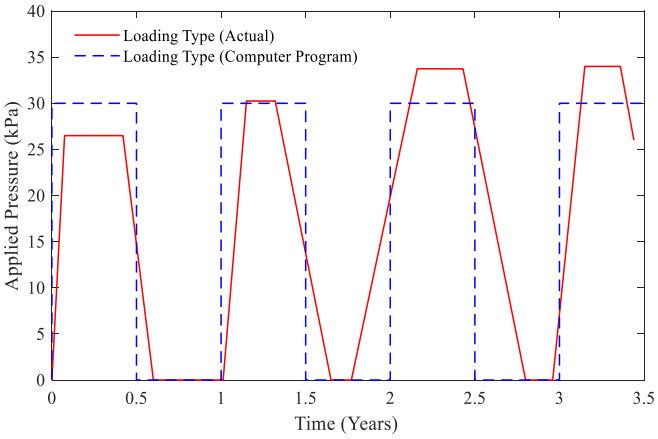


Figure 7 Difference between loading type used in the computer program and actual at the site of a full-scale silo built in Italy

For the heterogeneous layer case, to ensure that the flow conditions at the interface of the different layers can be satisfied, the finite difference results under a constant applied load are compared to that of the analytical solution by Schiffman and Stein (1970), and Figure 9 shows the comparison results, which are in good agreement.

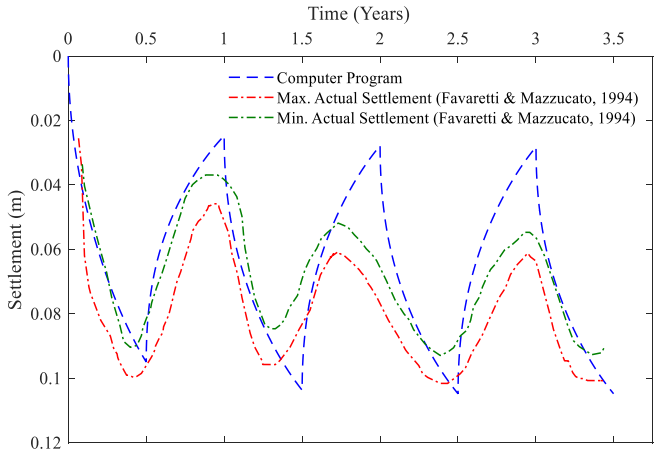


Figure 8 Comparison between finite difference analysis results and field monitoring records of a full-scale silo built in Ca'Mello near Porto Tolle (Italy) by Favaretti and Mazzucato (1994)

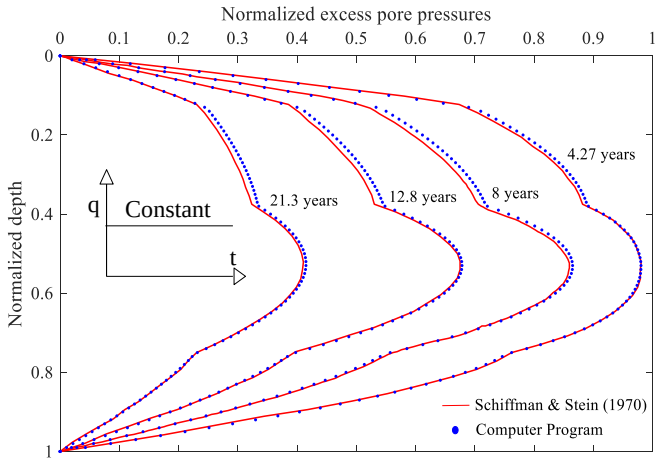


Figure 9 Comparison between results of the computer program and analytical solution by Schiffman and Stein (1970) for the heterogeneous layer under a constant applied stress

## 6. EXCESS PORE PRESSURES UNDER STEPPED CYCLIC LOADS

Immediately upon applying external stress, the positive excess pore pressures initially increase to the magnitude of maximum applied stress; during the entire loading period, the positive excess pore pressures dissipate. During unloading, the negative excess pore pressures are generated; the magnitude of these negative excess pore pressures depend on the gain in effective stresses until the last sub-time step of the loaded portion in the cycle, and these reduce in magnitude during the entire unloading period. After a huge number of cycles, when there is no further increase in the magnitudes of excess pore pressures, the steady-state condition can be defined. Figure 10 shows the distribution of steady-state excess pore pressures with depth under different time periods/frequencies of cyclic loads for the case of X = 0.5. As the time period decreases, the positive steady-state excess pore pressures increase while the negative steady-state excess pore pressures decrease. With the increase in positive steady-state excess pore pressures, the maximum steady-state average effective stress decreases, $U_{max,\ ss}$ decreases, while, with the decrease in negative excess pore pressures, $U_{min,\ ss}$ increases. For X = 0.5, the magnitudes of positive and negative steady-state excess pore pressures are equal to each other, with a difference in the signs only. For the case of X = 0.75, the magnitude of positive steady-state excess pore pressures is lesser than that of the magnitude of negative steady-state excess pore pressures. For X = 0.25, the magnitude of positive steady-state excess pore pressures is more than that of negative excess pore pressures, which means that the magnitudes of steady-state excess pore pressures are much affected by the "X" value.

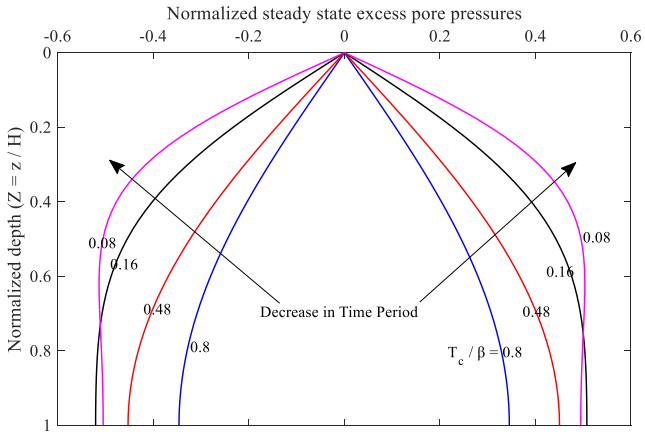


Figure 10 Distribution of steady-state excess pore pressures with depth under different time periods/frequencies of cyclic loads

## 7. STRESS STRAIN BEHAVIOR UNDER CYCLIC LOADING

Figure 11 shows the stress-strain behavior with a nonlinear inelastic model in which soil cyclically shifts from NC to OC state. With an increase in the number of cycles, under a given stress level, the soil's OC stress state becomes longer and longer, leaving the NC state shorter. After many cycles, the soil remains in OC state only and follows a constant stress-strain path repeatedly with loading and unloading.

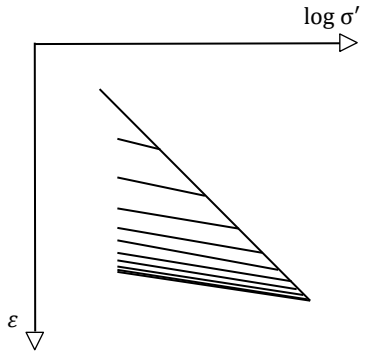


Figure 11 Stress-strain behavior under cyclic loading

## 8. VARIATION OF STEADY STATE DOC CALCULATED BASED ON SETTLEMENT WITH TIME PERIOD/FREQUENCY

Figure 12 shows the maximum and minimum steady state DOC results based on settlement ($U_{sett,\ ss}$) under different time periods of cyclic loads. Both Axes in Figure 12 are dimensionless and independent of stress level (stress level is the ratio of final effective stress to initial effective stress) and is applicable only for X = 0.5. For very long time periods/low frequencies of cyclic loads, the maximum steady-state DOC based on settlement ($U_{sett,\ maxss}$) is almost unity equivalent to under a monotonic load. Therefore, the $U_{sett,maxss}$ for very long time periods/low frequencies of cyclic loads, can be obtained using constant load theory. However, the minimum steady-state DOC based on settlement ($U_{sett,minss}$) is not equal to unity. Further, with the decrease in time period or the increase in frequency, both the $U_{sett,maxss,}$ and $U_{sett,minss}$ decrease. This decrease almost diminishes below a specific time period, and there is no significant decrease in both with a further decrease in time periods

of cyclic loads. The zone in which there is no further decrease in $U_{sett,maxss}$ and $U_{sett,minss}$ with a decrease in time period, is classified as "rapid zone" while the zone in which $U_{sett,maxss}$ is equal to one is termed as "slow zone". The zone in between slow and rapid is called as "transition zone" in which there is a significant drop in both $U_{sett, maxss}$ and $U_{sett, minss}$ with a decrease in the time period. Therefore, it can be summarized that the overall consolidation behavior can be separated into three zones under cyclic loads, i.e., slow, transition, and rapid.

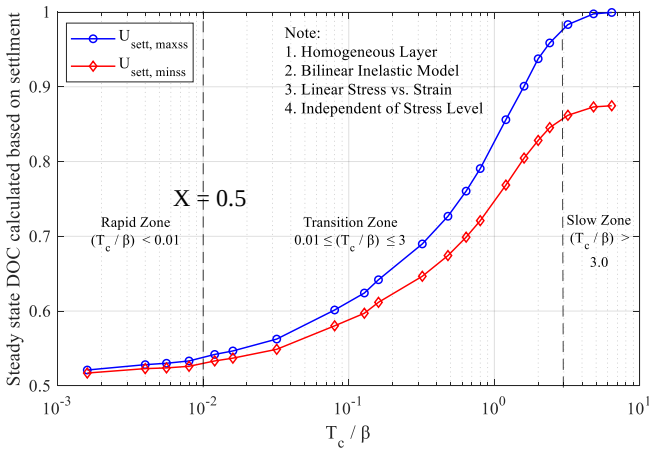


Figure 12 Variation of steady-state maximum and minimum DOC calculated based on the settlement at the surface with different time periods/frequencies of cyclic loads

The difference between $U_{sett,maxss}$ and $U_{sett,minss,}$ i.e., the difference between compression and rebound is large for long time periods/low frequencies of cyclic loads. However, the difference reduces by decreasing the time period. For very short time periods/high frequency, the difference is negligible; therefore, the compression and the rebound are almost the same. For long time periods/low frequencies of cyclic loads, more time is available for the positive and negative excess pore pressures to dissipate; thus, both positive and negative steady-state excess pore pressures are close to zero.

## 9. VARIATION OF STEADY STATE AVERAGE DOC CALCULATED BASED ON DISSIPATION OF EXCESS PORE PRESSURES WITH TIME PERIOD/FREQUENCY

For the linear elastic model, the maximum steady-state average DOC based on the dissipation of excess pore pressures and DOC based on the settlement are the same. However, there is a difference in the $U_{min,ss}$ and $U_{sett,minss}$ for all the time periods. Figure 13 shows the variation of $U_{max,ss,}$ and $U_{min,ss}$ with different time periods/ frequencies of cyclic loads for the case of X = 0.5. Both $U_{max,ss,}$ and $U_{min,ss}$ are almost equal to 0.5 in the rapid zone, showing that only 50% of the excess pore pressures dissipate under very rapid loading at the steady-state. The $U_{min,ss}$ is nearly zero under low frequencies of cyclic loads, and it increases with a decrease in the time period (or increase in frequency). Below a specific limit, i.e., in the rapid zone, there is no further increase in $U_{min, ss}$ with a further decrease in the time period of cyclic loads. For very long time periods/low frequencies of cyclic loads, the positive and negative excess pore pressures would have more time to dissipate; therefore, the steady-state positive and negative excess pore pressures are almost zero.

## 10. EFFECT OF CHANGE IN PERCENTAGE OF LOADED PORTION IN A CYCLE ON STEADY STATE DOC BASED ON SETTLEMENT AND AVERAGE STEADY STATE DOC BASED ON DISSIPATION OF EXCESS PORE PRESSURES

Figure 14 compares the maximum and minimum steady-state DOC based on the settlement for different "X" values and under different time periods of cyclic loads. Fig. 14 is developed using the bilinear inelastic model considering a linear stress-strain relationship. The X values considered were 0.25, 0.5, and 0.75. For a specific time period, the $U_{sett,ss}$ is small for a smaller X value and with the increase in X value, $U_{sett,ss}$ increases. When the loaded portion in a cycle is increased, the positive excess pore pressures would have more time to dissipate. Thus, the steady-state positive excess pore pressures are lesser, leading the steady-state maximum effective stresses to be more and settlements to be more. For higher X values, the magnitude of negative excess pore pressures is higher, increasing the minimum steady-state settlements. Similarly, for a smaller X value, the positive excess pore pressures have lesser time to dissipate; therefore, the steady-state excess pore pressures can be more, causing the steady-state effective stresses and settlements to be lesser.

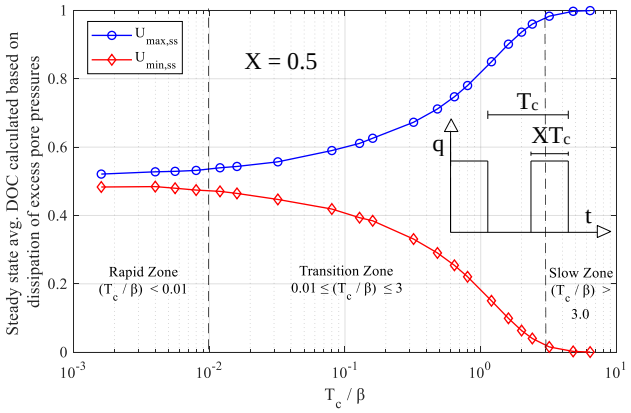


Figure 13 Variation of maximum and minimum steady-state average DOC calculated based on dissipation of excess pore pressures with time periods/frequencies of cyclic loads.

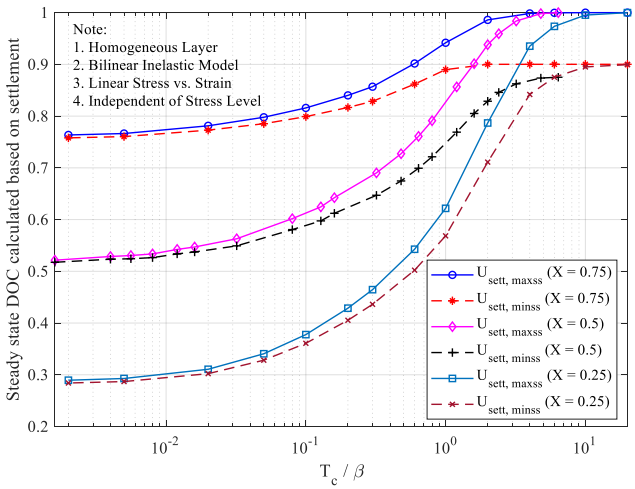


Figure 14 Comparison of maximum and minimum steady-state DOC calculated based on the settlement for different values of "X" under different time periods of cyclic loads.

Figure 15 shows the variations of maximum and minimum DOC based on the dissipation of excess pore pressures under different frequencies/time periods of cyclic loads for different X values. For larger X values, both have higher values at a particular time period, while for smaller values of X, the values are lesser.

## 11. EFFECTS OF STRESS LEVELS AND NONLINEAR STRESS STRAIN BEHAVIOR ON THE MAXIMUM STEADY STATE DOC CALCULATED BASED ON SETTLEMENT

The soil's actual behavior can be assessed more realistically by implementing the nonlinear $\sigma' \sim \varepsilon$ relationship. The consideration of linear $\sigma' \sim \varepsilon$ relationship is merely a simplification and should not be

used for high stress levels and very soft soils. Under cyclic loads, the nonlinear inelastic model is the most appropriate model, which is to be used in predicting the real soil behavior.

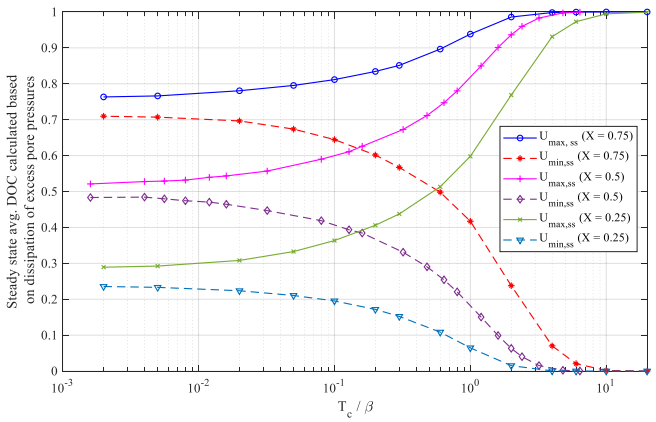


Figure 15 Comparison of maximum and minimum steady-state average DOC based on dissipation of excess pore pressures for different values of "X" under different time periods of cyclic loads

In this study, the nonlinear inelastic stress-strain model is adopted by varying the $m_v$ value with effective stresses or using the value of the compression ratio (CR) to calculate settlements. The decrease in $m_v$ with effective stresses is taken as proportional to the decrease in "k" with effective stresses; therefore, $c_v$ remains constant at any effective stress level. However, there is a variation of $c_v$ when the soil shifts from NC to OC range.

Figure 16 shows the analyses' results for the case of X = 0.25 - under stepped/square sine wave cyclic loads. Each curve represents the maximum steady-state DOC calculated based on settlement under a given stress level. It shows that for greater soil thickness, the soil layer should be divided into thin layers so that $\sigma_i'$ can be considered as constant with depth. Figure 16 shows the bilinear inelastic model (linear $\sigma' \sim \varepsilon$) and nonlinear inelastic model. It is clear that for a very low-stress level (i.e., small strain), the nonlinear inelastic model curve is very close to the bilinear inelastic model curve. It can be concluded that up to a certain stress level of about 1.1 (final effective stress is 10% more than the initial effective stress), the bilinear inelastic model with linear $\sigma' \sim \varepsilon$ relationship can give the results close to that of real soil behavior. However, it should be avoided at higher stress levels (large strain) as this model is independent of stress level and does not simulate the actual soil behavior. Figure 17 is the comparison for the cases of X = 0.25 and X = 0.75.

## 12. LIMITATIONS OF THE STUDY

Following are some of the limitations along with recommendations:

a) The study is entirely based on the numerical analysis; a detailed experimental and field observation should be carried out to verify the results of the proposed model.
b) The computer program is applicable only for a stepped/square wave cyclic load, which may differ from the actual cyclic loading.
c) The program does not consider the secondary compression /creep settlements.
d) The real nonlinear behavior with $c_v$, either increasing or decreasing with consolidation, should also be incorporated.

## 13. CONCLUSIONS

This study can be concluded/summarized as:

a) The consolidation behavior under cyclic loading is different from that under an instantaneously applied constant load. Under the cyclic loading, the degree of consolidation calculated based on settlements depends on cyclic load frequency and stress level.
b) After validation of the numerical code with analytical, experimental, and field monitoring data available in the literature, it can be concluded that the numerical code is well developed and can be used for the prediction and estimation of consolidation settlements for the practical problems in the field which subject the cyclic stresses on the subsoils.
c) The steady-state DOC based on settlement and steady-state average DOC based on dissipation of excess pore pressures decrease with a decrease in time periods of cyclic loads. Below a specific time period, there is no further decrease in both with a decrease in the time period.
d) With the increase in the X value for a specific time period, both steady-state DOC based on settlement and steady-state average DOC based on dissipation of excess pore pressures increase. In the rapid zone, i.e., for very short periods of cyclic loads, the steady-state average DOC value is approximately equal to the "X" value.
e) For linear stresses versus strains, the steady-state DOC based on the settlement is independent of the stress level. However, for nonlinear stresses versus strains, it increases with an increase in stress level. Moreover, the bilinear inelastic model can predict the actual nonlinear soil behavior up to a stress level of about 1.1.
f) The produced dimensionless plots/charts depict the complete picture of consolidation behavior under cyclic loads at different frequencies/time periods and stress levels. These plots can be used for the estimation of settlements under cyclic loads.
g) The current practice in the field to estimate the consolidation settlements of the problems that subject the subsoils to cyclic loading such as industrial silos, tanks, railway/highway traffic loading, is by using a constant applied load. This paper's theoretical investigations will help to understand and estimate the consolidation settlements under cyclic loadings of industrial silos, tanks, and railway/highway traffic loads.

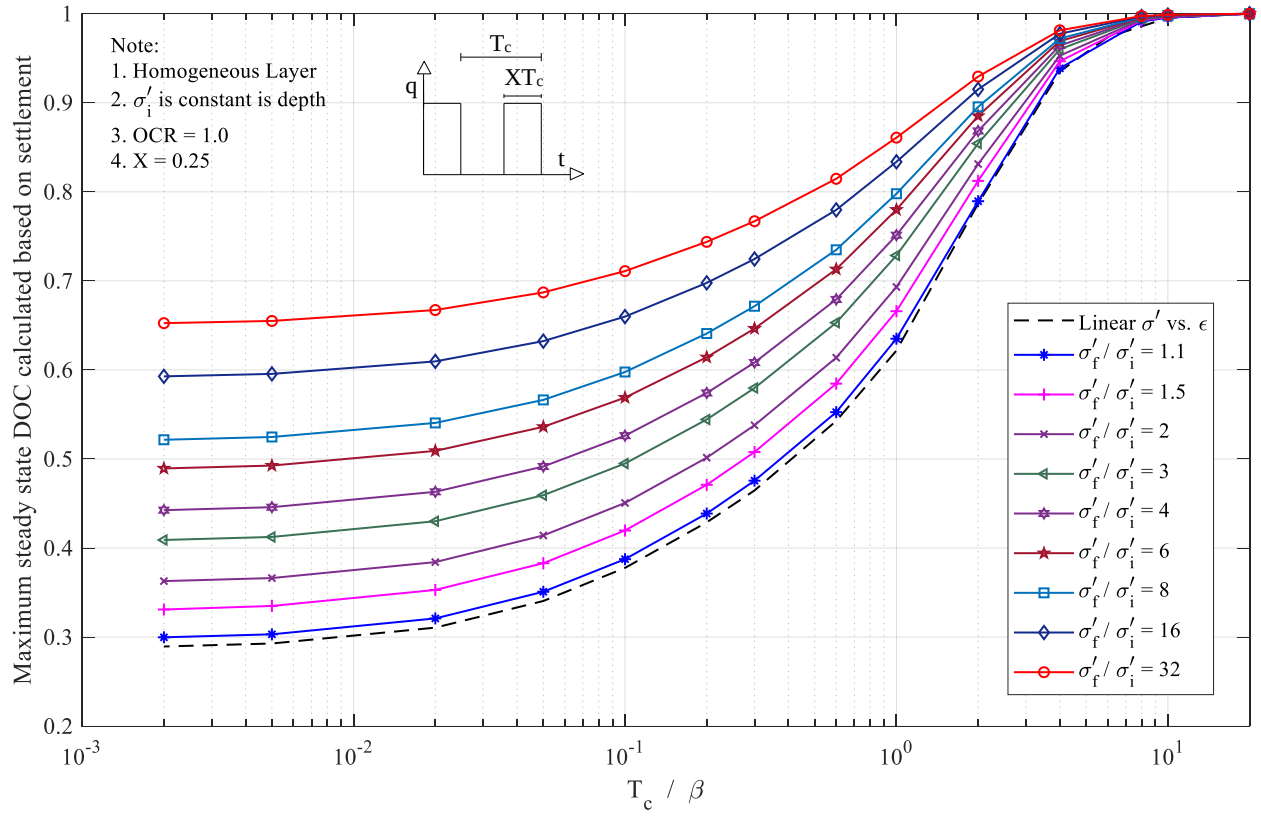


Figure 16 Variation of steady-state DOC calculated based on settlement under different time periods and stress levels for X = 0.25

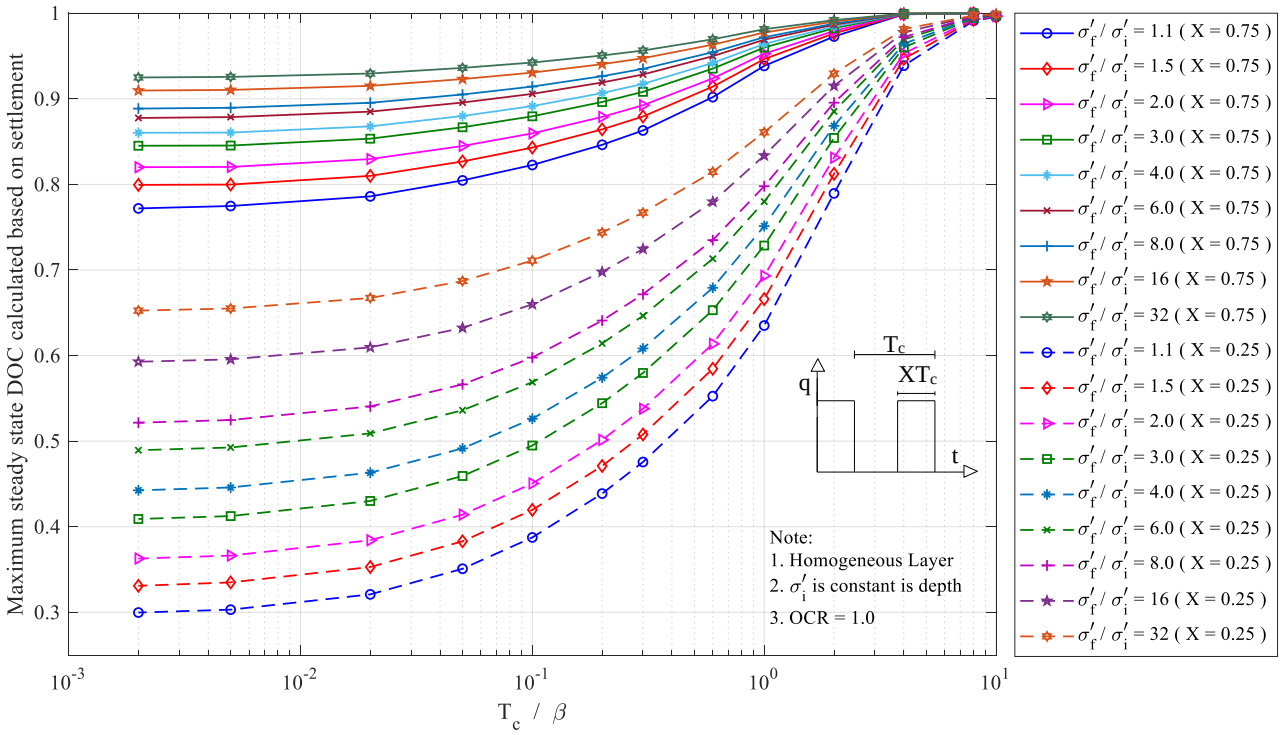


Figure 17 Comparison of maximum steady state DOC calculated based on settlement under different time periods and stress levels for X = 0.25 and X = 0.75

## 14. ACKNOWLEDGEMENTS

The authors are thankful to Prof. Noppadol Phien-Wej and Dr. Pham Huy Giao for their assistance and valuable comments during the manuscript's preparation.

## 15. NOTATIONS

| | |
|---|---|
| BCs | boundary conditions |
| $c_c$ | compression index (slope of virgin line in e vs. log σ' plot) |
| $c_k$ | permeability index (slope of e vs. log k) |
| CR | compression ratio (slope of virgin line in ε vs. log σ' plot) |
| $c_v$ | coefficient of consolidation in the vertical direction |
| DOC | degree of consolidation |
| k | coefficient of permeability in the vertical direction |
| $m_v$ | coefficient of volume change/compressibility |
| NC | normally consolidated |
| OC | over consolidated |
| OCR | over consolidation ratio |
| PW | pulse width (the loaded portion in a cycle) |
| RP | rest period (the unloaded portion in a cycle) |
| RR | recompression ratio (slope of rebound line in ε vs. log σ' plot) |
| $T_c$ | time period in terms of time factor calculated by using $c_v$ (NC) |
| $T_v$ | time in terms of time factor calculated by using $c_v$ (NC) |
| $U_{max, ss}$ | maximum steady-state average degree of consolidation based on dissipation of excess pore pressures |
| $U_{min, ss}$ | minimum steady-state average degree of consolidation based on dissipation of excess pore pressures |
| $U_{sett, maxss}$ | maximum steady-state average degree of consolidation calculated based on settlement |
| $U_{min, ss}$ | minimum steady-state average degree of consolidation calculated based on settlement |
| X | percentage of loaded portion in a cycle |
| α | ratio of $m_v$ (OC) to $m_v$ (NC) |
| β | ratio of $c_v$(NC) to $c_v$(OC) |
| $\sigma'_f$ | final effective stress |
| $\sigma'_i$ | initial stress level = initial effective overburden pressure |

## 16. REFERENCES

Baligh, M. M., and Levadoux, J. N. (1978) "Consolidation Theory for Cyclic Loading", Journal of Geotechnical Engineering Division, ASCE, 104(4), pp415–431.

Dei Svaldi, A., Favaretti, M., and Mazzucato, A. (2018) "Comparison Between Theoretical and Measured Settlements of a Cyclically Loaded Silo", Geotechnical and Geological Engineering, 36(2), pp1129–1143. https://doi.org/10.1007/s10706-017-0379-5

Duncan, J. M. (1993) "Limitations of Conventional Analysis of Consolidation Settlement" Journal of Geotechnical Engineering, ASCE, 119(9), pp1333–1359.

Favaretti, M., and Mazzucato, A. (1994) "Settlement of a silo subjected to cyclic loading", ASCE Specialty Conference Settlement 94, College Station, Texas, USA, pp775–785.

Favaretti, M., and Soranzo, M. (1995) "A simplified consolidation theory in cyclic loading conditions", In Proceedings of the International Symposium on Compression and Consolidation of Clayey Soils, A.A. Balkema, Rotterdam,The Netherlands, pp405–409.

Haq, S. (2018) "Numerical Analysis of Cyclic Consolidation of Saturated Clays", Masters Thesis, Asian Institute of Technology, Thailand.

Indraratna, B., Zhong, R., and Rujikiatkamjorn, C. (2016) "An Analytical Model of PVD-assisted Soft Ground Consolidation", Procedia Engineering, 143(Ictg), pp1376–1383. https://doi.org/10.1016/j.proeng.2016.06.162

Ladd, C. C., and Degroot, D. J. (2003) "Recommended Practice for Soft Ground Site Characterization: Arthur Casagrande Lecture". In 12th Panamerican Conference on Soil Mechanics and Geotechnical Engineering, Massachusetts Institute of Technology, Cambridge, MA USA, pp3–57.

Matsuda, H., and Shimizu, Y. (1995) "Laboratory tests of cyclic-load consolidation", Proc. of the 11th European Conference on Soil Mechanics and Found. Eng., 3, pp179-184.

Olson, R. E. (1977). "Consolidation Under Time-Dependent Loading", Journal of Geotechnical Engineering, ASCE, 103(1), pp55–60.

Phienwej, N., Thepparak, S., and Giao, P. H. (2005) "Prediction of differential settlement of buildings induced by land subsidence from deep well pumping". Geotechnical Engineering, 36(1), pp69–75.

Premchit, J. (1978) "Analysis and simulation of land subsidence with special reference to Bangkok", AIT Doctoral Dissertation No. D37, Asian Institute of Technology, Thailand.

Rahal, M. M. a., and Vuez, A. R. A. (1998) "Analysis of Settlement and Pore Pressure Induced by Cyclic Loading of Silo", Journal of Geotechnical and Geoenvironmental Engineering, 124(14790), pp1208–1210. https://doi.org/10.1061/(ASCE)1090-0241(1998)124:12(1208)

Schiffman, R. L. (1958) "Consolidation of Soil Under Time-Dependent Loading and Varying Permeability", Proceedings of the Thirty-Seventh Annual Meeting of the Highway Research Board, Washington, DC, 37, 584–617.

Schiffman, R. L., and Stein, J. R. (1970) "One-dimensional consolidation of layered soils", Journal of Soil Mechanics and Foundations Division, 96(4), pp1499–1504.

Seah, T. H., and Koslanant, S. (2003) "Anisotropic Consolidation Behavior of Soft Bangkok Clay", Geotechnical Testing Journal, ASTM, 26(3), pp1–11.

Terzaghi, K. (1943) "Theoretical Soil Mechanics", John Wiley and Sons, New York.

Toufigh, M. M., and Ouria, A. (2009) "Consolidation of inelastic clays under rectangular cyclic loading", Soil Dynamics and Earthquake Engineering, 29(2), pp356–363. https://doi.org/10.1016/j.soildyn.2008.03.006

Walker, R., Indraratna, B., and Rujikiatkamjorn, C. (2012) "Vertical drain consolidation with non-Darcian flow and void-ratio-dependent compressibility and permeability", Géotechnique, 62(11), pp985–997. https://doi.org/10.1680/geot.10.P.084

Wilson, N. E., and Elgohary, M. M. (1974) "Consolidation of Soils Under Cyclic Loading", Canadian Geotechnical Journal, 11(3), pp420–423. https://doi.org/10.1139/t74-042